Stability of the Microdroplets for Portable Biosensor

Yusuke Izawa, Toshihisa Osaki, Koki Kamiya, Satoshi Fujii, Norihisa Miki, and Shoji Takeuchi

***Abstract*— This paper highlights the behavior of microdroplets used for portable biosensors. Microdroplets have been applied for various Lab-on-a-chip applications, in which portability/wearable is becoming a trend word. However, the resonance (sloshing phenomena) of the microdroplets could be an issue. For example, bilayer lipid membrane, fragile characteristics due to its thickness of 5 nm, easily ruptures by jiggling. We therefore prepared various dimensions of droplets by changing the well shape, and examined the resulting waves depending on the vibration frequency between 20 and 100 Hz, including daily life frequencies. Moreover, we investigated an influence of surface coating of the wells by the same tests. The results of the first examination showed that the sloshing was effectively suppressed by reducing the well length along the vibration axis. We also found that the sloshing was suppressed by reducing surface energy of the microwells. We succeeded in clarifying the characteristics of microdroplets at the vibration in daily life frequency, which will be useful information for development of portable biosensors.**

I. Introduction

Cell membrane, consisting of a bilayer lipid membrane (BLM) and membrane proteins, encapsulates cytoplasm and controls substrates' transports in and out of cells. Recently, numbers of studies have been focused on developing bioinspired chemical sensors applying the cell membrane system. We have also demonstrated a concept of a portable BLM sensor [1], in which artificial BLM was integrated in a microdevice, named a double well chip (DWC), to use membrane protein for biosensors [2], [3]. The droplet contact method (DCM) was used for making stable BLM (Fig. 1) in DWC. Briefly, lipid-dispersed organic solvent was first infused in the wells. Then, aqueous solutions were added to the wells, which formed aqueous microdroplets surrounded by lipid monolayers. The droplets contacted each other, and artificial BLM was formed at the contiguous interface of the droplets. We have especially paid attention to ion channels as the sensor element, and succeeded in development of the chemical sensors for pesticides and cocaine [4], [5].

Portability is one of the important properties for the sensors for environmental monitoring and drug tests. Here, the fragile characteristics of BLM are the serious problem since BLM is sensitive to mechanical shock. We consider that there are two pathways for the BLM rupture in the DWC. One is that BLM is directly affected by the vibration. Aspinwall *et al.* explored the effect of surface energy of materials applied for BLM formation, revealing that the decrease of surface energy directly correlates with the improvement of electrical, mechanical, and temporal BLM stability [6]. Whitesides *et al.* revealed that the reduction of the pore that BLM is composed diameter below 40 μm mainly increased the stability of the planar bilayers, but had only a small effect on the level of the current noise [7]. Our previous studies also revealed that larger BLM area and the protein incorporation into BLM decrease the natural frequency of BLM. We succeeded in increasing robustness of BLM by decreasing BLM area and by mixing cholesterol in BLM [3], [8], [9]. The other pathway is that the force indirectly affects to BLM: When vibration is applied to the solutions surrounding BLM in DWC at the natural frequency, the resonance, i.e. sloshing of the solutions, occurs in the wells. The sloshing produces the pressure imbalance at the walls of the wells and easily causes the BLM rupture (Fig. 2). To develop portable BLM sensors, we believe that it is

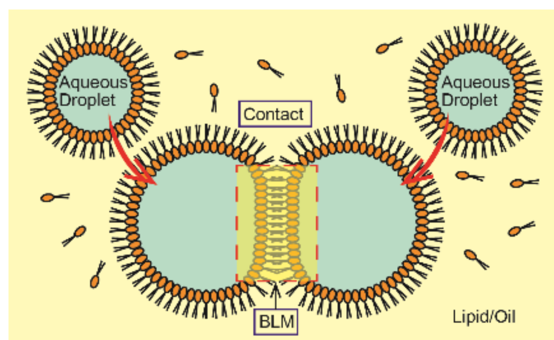

Figure 1. Droplet contact method. The BLM is formed at the contiguous interface between the two aqueous droplets.

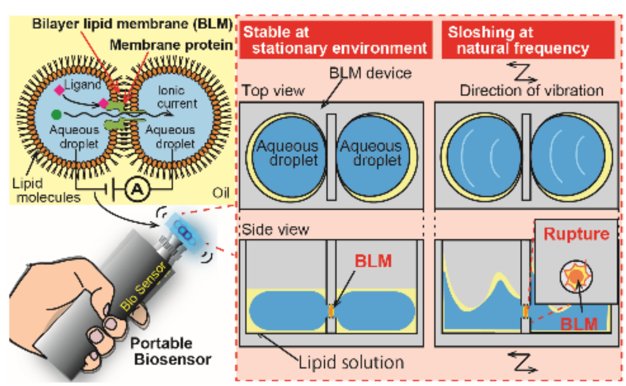

Figure 2. An artificial BLM system with the incorporation of membrane protein is a useful tool as a biosensor since the membrane proteins allow to transduce single molecule bindings to a large ionic current. However, vibration by an operator potentially causes the BLM rupture on a portable BLM biosensors due to the resonance (sloshing) of droplets.

*Research supported by KAKENHI (Grant Number 25246017) and the Regional Innovation Strategy Support Program of MEXT, Japan.

Y. Izawa, T. Osaki, K. Kamiya, S. Fujii, and S. Takeuchi are with Kanagawa Academy of Science and Technology (KAST), 3-2-1 Sakado Takatsu-ku, Kawasaki, Kanagawa 213-0012, Japan.

Y. Izawa, and N. Miki are with Department of Mechanical Engineering, Keio University, 3-14-1 Hiyoshi, Kohoku-ku, Yokohama, Kanagawa 223-8522, Japan.

S. Takeuchi is with Institute of Industrial Science, The University of Tokyo, 4-6-1 Komaba, Meguro-ku, Tokyo 153-8505, Japan (corresponding author: E-mail: takeuchi@iis.u-tokyo.ac.jp; Phone: +81-44-819-2037; Fax: +81-44-819-2092).

necessary to understand behavior of microdroplets under vibrations and to improve the vibrational stability of microdroplets.

In this study, we therefore aim to examine the sloshing phenomena of microdroplets in a well, and to stabilize the droplets under the vibrations at daily life frequencies for development of portable BLM sensors. We performed two kinds of vibration tests. One is to examine the behavior of a microdroplet infused in different diameters and shapes of microwells. The other is to investigate the influence of surface energy by using chemical modification of the well walls. The vibration frequency was set between 20 and 100 Hz that include daily life frequency (usually below 50 Hz).

II. Theory and Method

A. Housner's Equation

In this study, we used the Housner's equation, which theoretically predicts the natural frequency of solutions in a well by G. W. Housner [10], to determine the designs of the microwells. The natural frequency of a cylindrical well is written by the equation below.

$$f_n = \frac{1}{2\pi}\sqrt{\frac{\varepsilon_i g}{L}\tanh(\frac{\varepsilon_i H}{L})} \quad (1)$$

Table 1. Dimensions of microwells (unit: mm).

Cylindrical wells		Elliptical wells		
L	depth	*A*	B	depth
2	3.5	2	4	3.5
3		3		
4		4		
5		5		

L: diameter of a cylindrical wells.
A: length of an elliptical well, parallel to the vibrating direction.
B: length of an elliptical well, vertical to the vibrating direction.

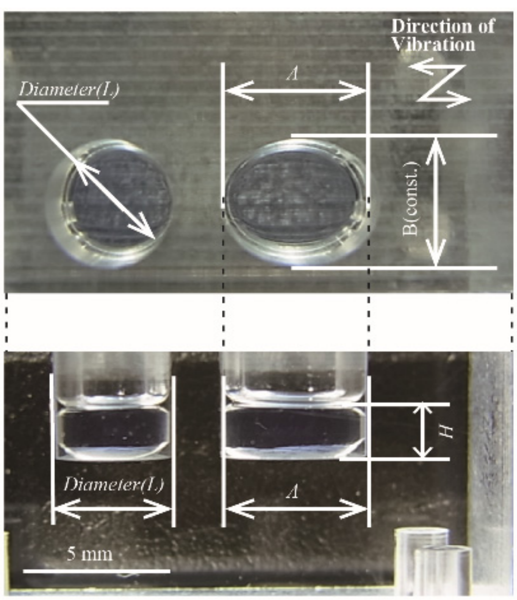

Figure 3. Top and side views of the wells. *L* is the diameter of the cylindrical wells, *A* and *B* are the parallel and vertical lengths of the elliptical well to the vibrating direction, respectively.

Here, f_n is the natural frequency of a cylindrical microwell, g is the gravitational acceleration, *L* is the diameter of the well, *H* is the height of the solution in the well. ε_i is zero points of the Bessel function of the first kind of the order *i*. The order *i* is the mode of the vibrating wave. According to this equation, it is clear that the natural frequency depends on *L* and *H*. In this study, we changed *L* as a parameter because the *L* has a larger impact to the natural frequency than *H* under the dimensions described in Table 1.

B. Designs of Microwells

We designed 7 types of microwells as shown in Table 1 and Fig. 3. The microwells were fabricated from an acrylic plate by micromachining.

C. Surface Characteristics of Microwells

We decreased surface energy of the well walls by using amphiphobic coating (SFE-B002H, AGC Seimi Chemical Co., Ltd.). First, the cylindrical well was dipped into the coating solution over 20 s. Then, the well was dried in the air over 30 min. The Contact angles at the coated and non-coated acrylic plates were measured using the sessile droplet method at three locations. 2 µL of H_2O and *n*-decane were manually deposited onto the surfaces, and the images of the droplets were taken by using a microscope. The contact angles were obtained by using a half-angle method.

D. Vibration Test

Fig. 4 shows the setup for the vibration test. In the well, we first infused the lipid solution (20 mg/mL Egg phosphatidylcholine in *n*-decane), and then added the buffer solution (1 M KCl, 10 mM phosphate buffer, pH 7.4). The volume was adjusted to be 3.5 mm in the depth for the different types of wells, and the volume ratio of the solutions was set at 1 to 7 (lipid to the buffer solution). The well was then loaded on the vibration stage that was horizontally moved by a shaker. A high-speed camera was used for imaging (1,000 fps). The vibration condition was 20–100 Hz with amplitude of 0.3 mm. We analyzed the wave heights from the videos by using ImageJ and determined the natural

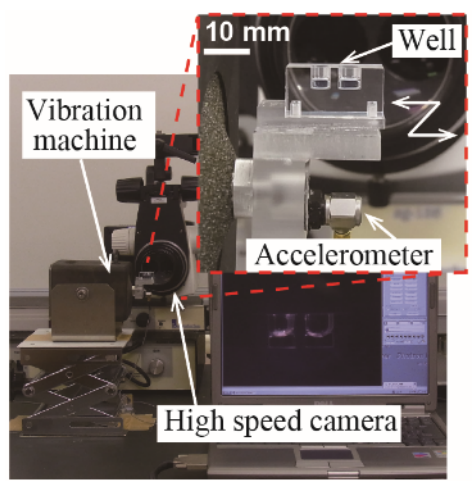

Figure 4. Setup for vibration test. Vibration between 20 and 100 Hz was horizontally added to the well by the machine. The movements were captured with a high-speed camera from a side of the well at 1,000 fps.

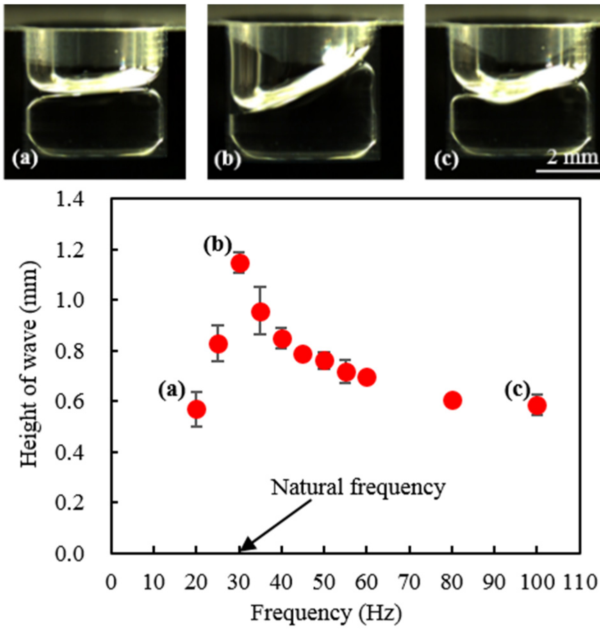

Figure 5. Wave height of microdroplets vs. vibration frequency for the cylindrical well (L = 4 mm). The images represent the behavior of vibrating microdroplets (a) 20 Hz, (b) 30 Hz (natural frequency), (c) 100 Hz. Error bars: standard deviation (N = 3).

frequency. From this data, we derived the mean value and a standard deviation (N=3).

III. Results and Discussion

A. Behavior of Droplets in Cylindrical and Elliptical Wells

Fig. 5 represents the wave heights of the droplet in a cylindrical microwell (L=4 mm) as a function of the applied frequency. Three images show the waves of the microdroplets at the respective frequencies. The frequency at the peak indicates the natural frequency. With the cylindrical well with 4 mm diameter, the natural frequency was 30 Hz, which is within daily life frequency.

Fig. 6 and 7 summarize the data of the vibration tests on the cylindrical and elliptical wells. Fig. 6 represents the natural frequency against L and A. The natural frequencies for the different shapes of the wells showed the same trend. This result indicates that the length vertical to the vibrating direction hardly affected to the natural frequency. The decrease of L and A increased the natural frequency, and shifted up to 55 Hz from 25 Hz with the deformation of the well shape. Fig. 7 represents the maximum height of wave against L and A. The decrease of L and A suppressed the wave height. However, the slopes between the cylindrical and elliptical wells were slightly different. We consider that this difference was due to the difference of the solution volumes caused by the parameter B (4 mm, constant). The kinetic energy of the solution by the vibration increased with the increase of the volume. Both graphs in Fig. 6 and 7 were in qualitative agreement with the Housner's equation.

These results suggest the following. First, the natural frequency of microdroplets is shifted to a higher frequency without changing the volume by the increase of A and the decrease of B. Second, it is possible to suppress the wave height by decreasing B, the well length vertical to vibrating direction, without changing the natural frequency.

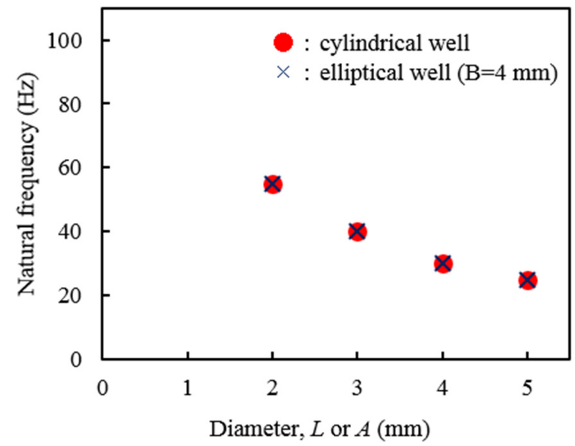

Figure 6. Natural frequency vs. L or A on two different well shapes. L is the diameter of the cylindrical well; A is the well length parallel to the vibrating direction. Red circle: cylindrical wells. Black cross: elliptical wells.

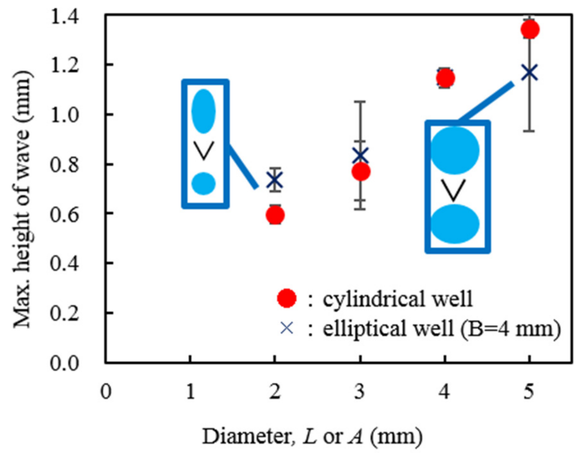

Figure 7. Max. wave height vs. L or A on two different well shapes. L is the diameter of cylindrical well; A is the well length parallel to the vibrating direction. Red circle: cylindrical wells. Black cross: elliptical wells. Error bars: standard deviation (N=3).

Table 2. Contact angles on each substrate (unit: °).

	Clean acrylic	**Coated acrylic**
H_2O	72±4	108±5
***n*-decane**	>10	61±3

B. Behavior of Droplets in Coated and Non-coated Wells

First, we confirmed the contact angles of the amphiphobic coated and the non-coated acrylic plate, shown in Table 2. The surface property of the non-coated plate was weakly hydrophobic and strongly oleophilic; the contact angles were approximately 70 degrees at water and below 10 degrees at *n*-decane. On the other hand, the property of the coated plate was strongly amphiphobic; the contact angles were approximately 110 degrees at water and 60 degrees at *n*-decane. In the vibration tests, the results suggest that the natural frequencies of the droplets at the coated wells were higher than those of the non-coated wells, and the maximum height of wave of the droplet was considerably suppressed for the droplets in the coated well. Importantly, the natural frequencies and the maximum height of wave changed without changing the well shapes. This result was not expected by the Housner's equation because the theory, which is often applied to the sloshing in a gigantic tanks, does not take into account the viscosity and the surface tension at the walls, which become important in micrometer scales. In this experiment, the viscosity should be the same for both coated and non-coated wells since the same conditions were used for the both wells. Therefore, it was considered that the deviation was due to the increase of fractional resistance between solution and well. A previous work reported that the perfluorinated coating enlarges the fractional resistance [11]. This result suggests that the surface coating would significantly affect to the behavior of the microdroplets in microwells.

IV. Conclusion

In this study, we experimentally demonstrated the sloshing of microdroplets in wells with various shapes and surface characteristics. By decreasing the well diameter *L*, we were able to shift the natural frequency up to 55 Hz and to suppress the wave height. We also found that the decrease of surface energy of the microwells suppressed the wave height.

We presented a few directions to control the natural frequency and wave height of microdroplets in the well. Further study will provide practical device designs for portable droplet-based biosensors.

Acknowledgment

We thank to Mses. Maiko Uchida, Yoshimi Nozaki, Yumi Kagamihara, Sora Hashino, and Chikako Minami (KAST) for their kind assistance. This work was partly supported by KAKENHI (Grant Numbers 25246017) and the Regional Innovation Strategy Support Program, MEXT, Japan.

References

[1] R. Kawano, T. Osaki, H. Sasaki, M. Takinoue, S. Yoshizawa, and S. Takeuchi, "Rapid detection of a cocaine-binding aptamer using biological nanopores on a chip," *J. Am. Chem. Soc.*, vol. 133, no. 22, pp. 8474–8477, 2011.

[2] K. Funakoshi, H. Suzuki, and S. Takeuchi, "Lipid Bilayer Formation by Contacting Monolayers in a Microfluidic Device for Membrane Protein Analysis," *Anal. Chem.*, vol. 78, no. 24, pp. 8169–8174, Dec. 2006.

[3] R. Kawano, Y. Tsuji, K. Sato, T. Osaki, K. Kamiya, M. Hirano, T. Ide, N. Miki, and S. Takeuchi, "Automated Parallel Recordings of Topologically Identified Single Ion Channels," *Sci. Rep.*, vol. 3, p. 1995, Jun. 2013.

[4] R. Kawano, Y. Tsuji, K. Kamiya, T. Kodama, T. Osaki, N. Miki, and S. Takeuchi, "A Portable Lipid Bilayer System for Environmental Sensing with a Transmembrane Protein," *PLoS One*, vol. 9, no. 7, p. e102427, Jul. 2014.

[5] A. Nobukawa, T. Osaki, T. Tonooka, Y. Morimoto, and S. Takeuchi, "Electrical detection of pesticide vapors by biological nanopores with DNA aptamers," in *Proceedings of IEEE MEMS*, 2015, pp. 596–599.

[6] L. K. Bright, C. A. Baker, M. T. Agasid, L. Ma, and C. A. Aspinwall, "Decreased aperture surface energy enhances electrical , mechanical , and temporal stability of suspended lipid membranes," *ACS Appl. Mater. Interface*, vol. 5, pp. 11918–11926, 2013.

[7] M. Mayer, J. K. Kriebel, M. T. Tosteson, and G. M. Whitesides, "Microfabricated Teflon Membranes for Low-Noise Recordings of Ion Channels in Planar Lipid Bilayers," *Biophys. J.*, vol. 85, no. 4, pp. 2684–2695, Oct. 2003.

[8] R. Kawano, T. Osaki, H. Sasaki, and S. Takeuchi, "A polymer-based nanopore-integrated microfluidic device for generating stable bilayer lipid membranes," *Small*, vol. 6, no. 19, pp. 2100–2104, 2010.

[9] L. N. S. Zaleha, T. Osaki, R. Kawano, K. Kamiya, N. Miki, and S. Takeuchi, "Robustness of Suspended Bilayer Lipid Membrane," in *Proceedings of Micro TAS*, 2014, pp. 701–702.

[10] G. W. Housner, "Earthquakes Pressures on Fluid Containers." 1954.

[11] M. Sakai, J. H. Song, N. Yoshida, S. Suzuki, Y. Kameshima, and A. Nakajima, "Direct observation of internal fluidity in a water droplet during sliding on hydrophobic surfaces," *Langmuir*, vol. 22, no. 11, pp. 4906–4909, 2006.